Environmental impact of high power density microwave beams on different atmospheric layers

T. R. Robinson, T. K. Yeoman and R. S. Dhillon,

Radio and Space Plasma Physics Group, Department of Physics and Astronomy,
University of Leicester, Leicester LE1 7RH, UK.

ESA Contract number: 18156/04/NL/MV

Environmental impact of high power density microwave beams on different atmospheric layers

T. R. Robinson, T. K. Yeoman and R. S. Dhillon,

Radio and Space Plasma Physics Group, Department of Physics and Astronomy, University of Leicester, Leicester LE1 7RH, UK.

ESA Contract number: 18156/04/NL/MV

Department of Physics and Astronomy, University of Leicester, Leicester LE1 7RH, UK.

Francesco Cattaneo
Andres Galvez
Leopold Summerer

Radio and Space Plasma Physics Group Tech. Rep. 63, Leicester University, UK, 2004.

University of Leicester

September 2004

Abstract

The mechanisms involved in the trans-ionospheric propagation of Solar Power Satellite microwave beams are considered in the context of both efficiency of the power transfer as well as of environmental impact. Processes involved include, linear effects such as collisional absorption, scintillation and scattering which lead to loss of energy from the beam, as well as the excitation of certain nonlinear effects, such as stimulated scattering and the thermal self-focussing instability. The results of predictions of simple analytic theories of the threshold powers required to excite these instabilities are also discussed in relation to the results of various experimental findings. Further, environmental impact effects associated with the heating of the ionosphere by the microwave beam are dealt with. The effects of heating on ionospheric electron temperature, neutral temperature, electron density and chemical concentrations of atmospheric gases are estimated quantitatively. Finally, limitations in current knowledge concerning all of these effects are considered.

Table of contents

1. Introduction

Solar Power Satellites (SPS) and related systems are an attractive way of exploiting the huge quantities of energy available in the form of solar radiation and converting it into useful energy at the Earth's surface. Although the technological aspects of this concept are fairly well defined, the effects of trans-ionospheric propagation of the microwave beams, which is essential to SPS operation, are less well understood. The aim of this short report is to identify the key mechanisms that lead to the degradation of the quality of SPS operations and also those that may lead to potential environmental impact effects, and to identify key data bases needed to evaluate these effects.

The SPS concept as a means of converting the visible parts of the solar radiation spectrum into useful energy at the Earth's surface has been around for several decades (Glaser et al., 1998). These and similar systems essentially comprise a space platform that supports an energy transducing system to convert solar radiation into microwaves, together with a high power microwave transmitter and beam-forming antenna that enables the microwaves to be efficiently focussed at a ground-based receiver. Whilst the technical design aspects of such a system are pretty well defined (e.g. Summerer et al., 2003), the implications of the transmission of high power density microwaves through the intervening ionosphere are less predictable. This lack of predictability arises from several factors. Firstly, although the basic mechanisms involved in electromagnetic wave propagation through collisional plasma, like that in the Earth's ionosphere, are well understood, calculations based on mean ionospheric conditions are totally inadequate.

The reason is that the ionosphere is highly variable, often in unpredictable ways, on a variety of spatial and temporal scales (Robinson and Leigh, 1987; Robinson and Beard, 1995). Even empirical models, such as the International Reference Ionosphere (IRI) that take account of diurnal and solar cycle variations cannot capture the full picture of the numerous ephemeral effects such as those due to solar flares and magnetospheric storms (Yeoman et al., 1990). A brief overview of the structure and properties of the ionosphere is given in the Appendix.

A second potential reason for unpredictable behaviour is that at high power densities such as those encountered in SPS systems interactions between the electromagnetic waves and the ionospheric plasma can trigger instabilities that involve nonlinear feedback processes. Such nonlinear effects can lead to significant modification of the ionospheric plasma which in turn causes modification of the beam itself. Although the conditions for the onset of nonlinearity can be predicted, the final state of a strongly coupled beam-plasma system may be intrinsically unpredictable.

Below, the basic mechanisms that govern the interaction of electromagnetic waves and the ionospheric plasma that could impact on the efficiency of microwave power transmission are outlined. These include linear phenomena, such as absorption due to electron collisional effects and scintillation and scattering due to the presence of plasma density irregularities, that are independent of the amplitude of the electromagnetic waves. Because the ionosphere is an extremely variable medium, both normal and extreme conditions under which these

linear processes operate will be considered. In addition, potentially important nonlinear interactions between high power electromagnetic modes and the ionospheric plasma will also be dealt with. The reliability of quantitative predictions of SPS performance that are affected by all of these processes are also assessed by identifying gaps in current knowledge, such as lack of data and lack of understanding of fundamental processes.

2. Linear processes affecting power transmission through the ionosphere

The amplitude and coherence of electromagnetic beams traversing the ionospheric plasma can be affected by three main linear processes. These are refraction due to plasma density dependent phase speeds, absorption due to electron collisional effects and scattering and scintillation due to diffraction in the presence of a spectrum of naturally occurring plasma density irregularities. At the L-band operating frequencies of SPS microwave transmissions (2.48 GHz and 5.8 GHz), the first two of these processes, under normal conditions, are expected to have minimal effects on the amplitude and direction of the electromagnetic beam. Even under extreme conditions, refraction is never likely to be a problem in disturbing the direction of the beam. However, some extreme conditions give rise to enhanced and highly variable levels of absorption that can lead to fluctuating power loss before the microwaves reach the ground receivers, so the basics of the absorption process are outlined in a subsection below. The results are also applied, in a later subsection that deals specifically with extreme conditions. The third linear mechanism above, i.e. diffractive scattering and scintillation is known to regularly affect L-band trans-ionospheric transmissions, such as those utilised in communications and navigation satellites. These effects cause significant fluctuations in the amplitude and phase of such signals and lead to power being scattered out of the geometric beam. This mechanism will also be dealt with in this section.

In the next subsection, collisional absorption in dealt with. This arises in the ionospheric plasma due to collisions between electrons and heavier neutral particles and ions. After outlining the calculation of collisional absorption, absorption levels for typical ionospheric conditions are evaluated. This is followed by calculations corresponding to two situations when absorption levels could exceptionally be enhanced above those normally expected. These are (i) when the ionosphere is modified by charged particles from coronal mass ejections from the Sun and (ii) when the lower ionosphere is strongly heated by a lightning flash, which enhances electron collisional effects by several orders of magnitude.

2.1 Collisional absorption

The non-deviative absorption coefficient *A*, expressed as the fractional power loss in decibels (dB) for an electromagnetic wave of angular frequency ω_0 is given by the following integral (Davies, 1990) along a path length *s*,

$$A = -4.34 \int \kappa ds \tag{2.1}$$

where

$$\kappa = \frac{{\omega_p}^2 \nu_e}{{\omega_0}^2 c} \tag{2.2}$$

and

$$\omega_p{}^2 = \frac{N_e e^2}{\varepsilon_0 m_e}. \tag{2.3}$$

Here ω_p is the angular plasma frequency of the ionosphere, ν_e is the electron collision frequency, N_e is the electron density, m_e is the electron mass, e is the electronic charge, ε_0 is the permittivity of free space and c is the speed of light in a vacuum. In general, N_e and ν_e are implicitly dependent on s, particularly through the vertical stratification of atmosphere and ionosphere (see sub-section 2.1.1 for details). The other parameters on which κ depends, in relations (2.1) to (2.3), may be taken as constant. Non-deviative absorption applies to conditions under which $\omega_0 >> \omega_p$, which is the case for SPS operating frequencies everywhere in the Earth's ionosphere. It implies that there is no refraction of the electromagnetic waves and that they propagate along straight ray paths. This greatly simplifies the calculation in (2.1). Relations (2.1) to (2.3) indicate that, for a given wave frequency, the absorption level is controlled by the product of the electron density and the electron collision frequency in the ionosphere, whose variation with altitude above the Earth's surface under normal conditions is described in the following sub-section.

2.1.1 Normal conditions

Under normal conditions, i.e. in the absence of geomagnetic and solar disturbances, the absorption effects on the SPS beam would be expected to be extremely small. Using the electron density and collision frequency input data in Fig. 1 it is clear from Fig. 2 (dashed curve) that over 99.7% of SPS microwave power remains after traversing the entire ionosphere and atmosphere. Thus absorption levels under normal ionospheric conditions are very low. Notice also from Fig. 2 that most of the absorption takes place in the lower ionosphere.

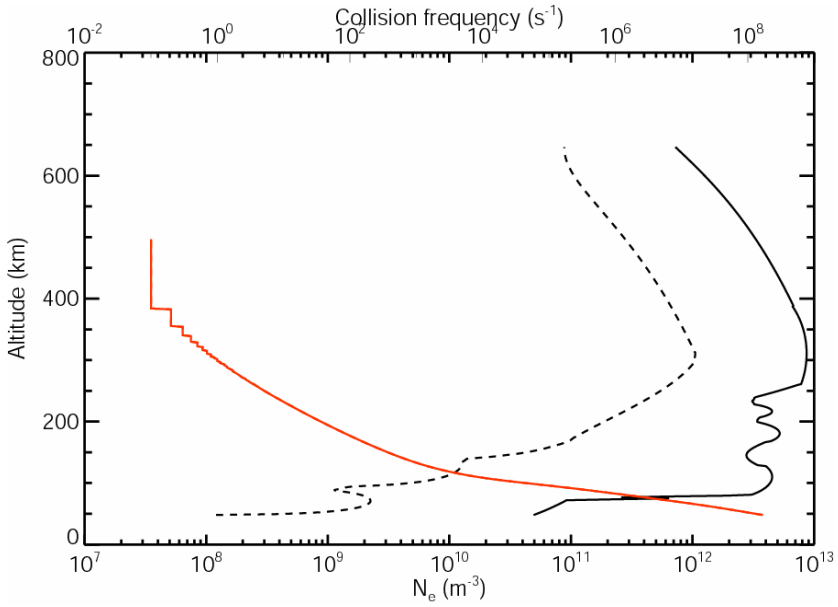

Figure 1 Electron collision frequency (red), normal electron density (dashed) and electron density (black) enhanced by CME event, against altitude.

2.1.2 Extreme conditions

2.1.2.1 Coronal mass ejection events

During late October 2003 a coronal mass ejection (CME) event occurred which strongly enhanced the electron density in the ionosphere. This was observed by the European Incoherent Scatter (EISCAT) Radar facility located in Scandinavia. The event lasted for over 24 hours and produced highly variable conditions in the ionosphere. Using one of the extreme density profiles from the EISCAT radar, illustrated in Fig. 1, the absorption levels for a 2.48 GHz signal were recalculated. The absorption levels under the enhanced conditions were now found to be significant, with only just over 80% of the SPS beam power reaching ground level, as indicated in Fig. 2 (solid curve).

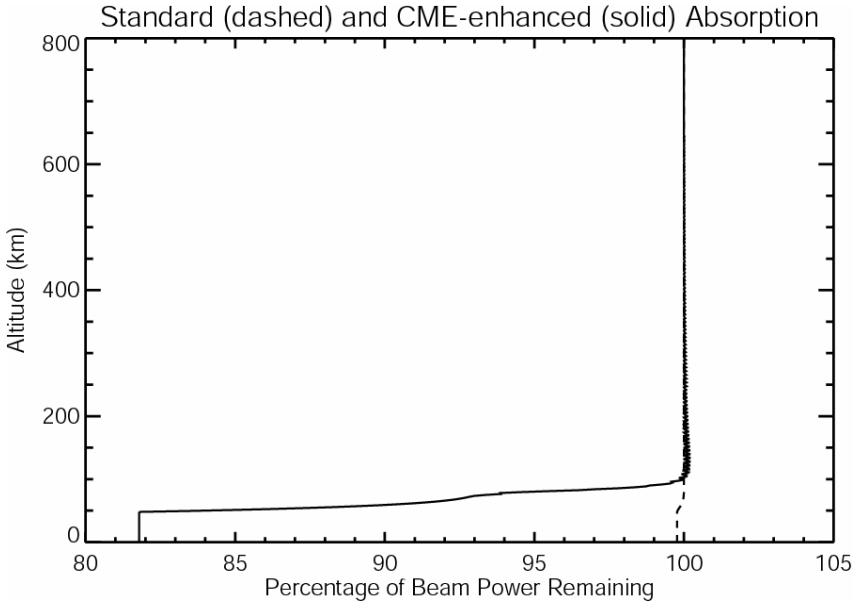

Figure 2 Percentage power remaining against of altitude for a down-coming electromagnetic wave of frequency 2.48GHz. The dashed curve represents normal conditions and the solid curve those enhanced by CME event, corresponding to the data in Fig. 1.

2.1.2.2 Lightning

Inan et al. (1991) have modelled the effects of lightning flashes on the lower ionosphere where most of the collisional absorption occurs. These authors found that the lightning increased the electron temperature in the lower ionosphere to values in excess of 30,000 K. This increased the electron collision frequency in a roughly 10 km thick layer in the lower ionosphere by a factor of about 400. This has the effect of increasing the contribution of this layer to the integral in (2.1) by this huge factor. Calculations similar to those for the CME case above lead to estimates of enhanced absorption levels during lightning discharges. However, even under the most extreme conditions associated with lightning, it is estimated that no more than about 3% of the power is lost due to these effects.

2.2 Scattering and scintillation

It is very well known that electromagnetic waves propagating between space platforms located above the ionosphere and the ground suffer varying degrees of amplitude and phase scintillation due to diffractive effects brought about by the spatially and temporally varying plasma refractive index of the ionosphere. This variation takes the form of plasma density irregularities that, due to anisotropic plasma transport in the presence of the geomagnetic field, tend to be strongly elongated along the geomagnetic field direction. The spatial scales of these irregularities across the geomagnetic field range from a few metres to several tens of kilometres. They have been intensively studied in the context of communications and navigation satellite systems because of the errors that scintillations can cause in these important systems. Fig. 3 shows an example of the levels of signal amplitude fading that are caused by these variations in plasma density, as indicated by the total electron content (TEC) parameter (upper panel), in various L-band signals propagating through the associated ionospheric plasma density irregularities between geostationary satellites and ground stations in Japan.

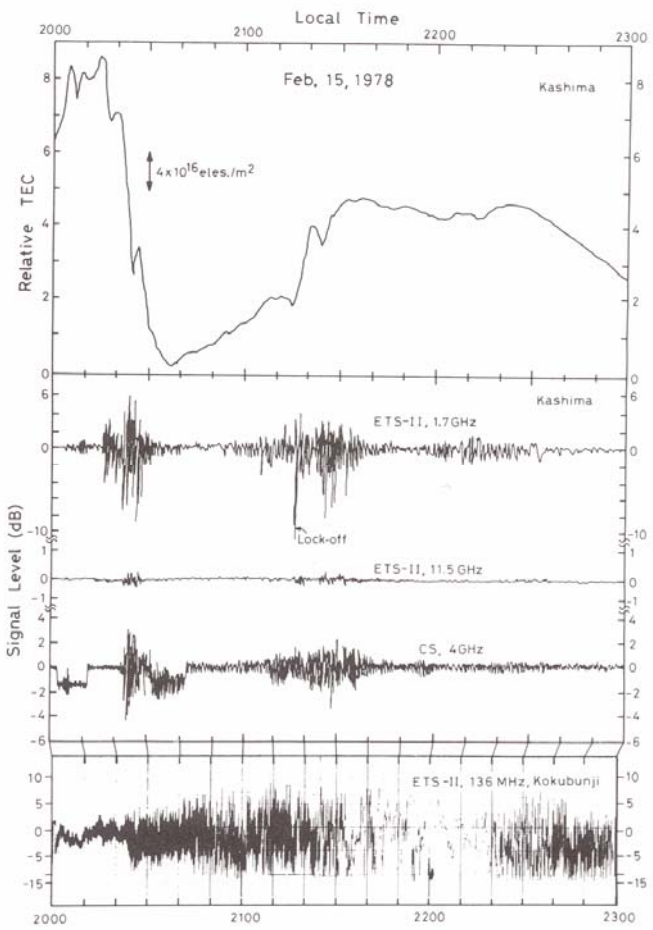

Figure 3 Scintillation on 136 MHz, 1.7 GHz, 4 GHz and 11.5 GHz on ground to satellite links over Japan, together variations in total electron content (TEC) in upper panel (From Ogawa et al., 1980).

It should be stressed that the conditions pertaining to the data in Fig. 3 were associated with a geomagnetic storm which produced particularly severe scintillation effects. However

these conditions are not uncommon. They are more likely to occur during periods of high sunspot number as indicated schematically in Fig. 4.

Fig. 4 also illustrates that the most severe scintillation effects occur in the low-latitude regions around dusk and in the polar regions. The former are due to the preferential excitation of the Rayleigh-Taylor instability where the geomagnetic field is almost horizontal and the latter are due to coupling between the geomagnetic field lines and the dynamic magnetic field in the solar wind. However, the likelihood of scintillation effects occurring is greatly enhanced during periods of geomagnetic disturbances at all latitudes and times. There is no reason to believe that amplitude fluctuations at levels similar to those illustrated in Figs. 3 and 4 will not also occur in SPS due to these natural ionospheric effects. This would imply that an SPS beam operating at 2.48 GHz would have to be able to cope with amplitude variations of up to 10 dB on time scales of seconds. This implies variations amounting to an almost total loss of power to a doubling of power within the period of a few seconds. It also implies that power will be diffracted out of the geometrical beam and could impact the ground outside the designated collecting area. For example, Davies (1990) describes modelling of this spreading for a localised density variation in the ionosphere. This indicated diffractive spreading at ground level of up to 10 km for transionospheric L-band signals. Operating at 5.8 GHz could significantly reduce the effect of scintillations and diffractive spreading of the beam since the effect decreases with increasing operating frequency (as illustrated in Fig. 3).

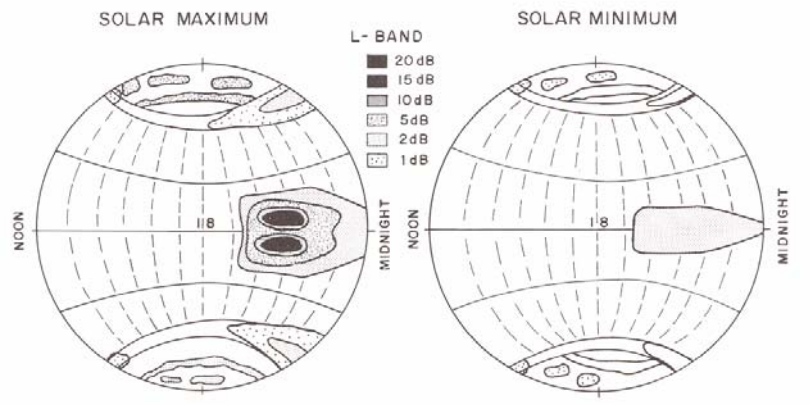

Figure 4 Global distribution of worst case amplitude fading levels at L-band frequencies during high and low sunspot conditions (From Basu et al. 1988).

Major population centres such as Japan and India lie within the region which would be most severely affected by scintillations on SPS systems. However, Western Europe lies in the mid-latitude region which is less affected by scintillation problems, except under the most severe conditions, which occur rather infrequently. On the other hand the occurrence of scintillation effects is highly unpredictable due to the variable nature of the solar-terrestrial plasma environment. This environmental variability is now usually referred to as “Space Weather”. There is considerable international research effort currently being

focussed at improving our ability to predict space weather. However it is quite likely that the solar-terrestrial system is subject to chaotic behaviour and is intrinsically unpredictable.

3. Nonlinear processes

The linear effects discussed above occur for electromagnetic waves of any power. In this section nonlinear effects which depend for their efficacy on the power density of the electromagnetic waves and which may prove of importance in the SPS context will be considered. These effects involve the interaction between a high power electromagnetic wave or 'pump' and naturally occurring ionospheric plasma waves which may be electromagnetic (EM) or electrostatic (ES) in nature. Below, three of the most important and well-understood are outlined. The first two involve the scattering which is enhanced and eventually becomes unstable due to nonlinear ponderomotive forces (Fejer, 1979). These can lead to loss of power from the SPS beam due to conversion of power to ES waves which remain in the ionosphere. This not only leads to a reduced efficiency in transferring solar power to the ground, but the extra (anomalous) absorption due to nonlinear interactions can cause much stronger heating of electrons than is expected due to (linear) collisional absorption, treated in section 2. The impact of electron heating and its consequences on such things as electron density and ionospheric chemistry will be dealt with in a later section.

The third type of nonlinear interaction, the self-focussing instability (Perkins and Goldman, 1981), which may turn out to be the most important in the SPS context, involves nonlinearity due to collisional heating. This leads to the generation of plasma density irregularities which cause scintillations of the SPS beam even when no natural scintillations, such as those discussed in section 2.2 above, are present. All three nonlinear mechanisms may lead to detrimental environmental effects in addition to degradation of the SPS beam and plasma heating. These further effects will include the generation of plasma waves and irregularities which can scatter any electromagnetic waves passing through the SPS beam, and thus create unwanted interference in communications, navigation and broadcasting signals (Rush, 1981). It is important to know what power thresholds are required to trigger these instabilities. Whilst these thresholds, which are evaluated below, are fairly well known, the nonlinear development and ultimate state of the waves and the ionospheric medium are largely unknown. From the data available (Summerer et al., 2003), the SPS beam is assumed to have a power flux of a few times 100 W m^{-2}.

3.1 Stimulated Brillouin scattering (SBS)

This mechanism involves the nonlinear interaction of the EM pump and scattered EM and ion acoustic (ES) waves. Ion acoustic waves propagate at the ion sound speed which is typically a few hundred m s^{-1} in the ionosphere and have frequencies well below the ionospheric plasma frequency, which is typically a few MHz. The threshold power flux level required to excite this process is given by (Fejer, 1979)

$$P_{th}(Wm^{-2}) = (0.017Wm^{-2})(T_i/1000K)(f/1.0GHz) \tag{3.1}$$

where T_i is the ion temperature in the ionosphere and f is the EM pump frequency in GHz. Under typical conditions in the upper ionosphere of T_i = 1000 K and at 2.48 GHz, the

power threshold is only 0.04 W m^{-2} and so the SBS should be strongly excited by the SPS beam.

3.2 Stimulated Raman scattering (SRS)

This mechanism involves the nonlinear interaction of the EM pump and scattered EM and electron acoustic (ES) waves. Electron acoustic waves propagate at the electron sound speed which is typically a few tens of km s^{-1} in the ionosphere and at frequencies just above the local plasma frequency. The threshold power flux level required to excite this process is given by (Fejer, 1979)

$$P_{th}(Wm^{-2}) = (4 \times 10^{-5} Wm^{-2})(N_e / 10^{12} m^{-3})^{1/2} (1.0GHz / f) \tag{3.2}$$

Under typical ionospheric conditions with the electron density at 10^{12} m^{-3}, the power flux threshold is only 0.000016 W m^{-2}. This again will be strongly excited in the ionosphere by the SPS.

3.3 Thermal self-focussing instability (TSI)

This process was extensively studied in the context of SPS in the early 1980s (e.g. Duncan, 1981; Perkins and Goldman, 1981), in relation to potential environmental impact effects. The power flux threshold given by Duncan (1981) for the TSI is

$$P_{th}(Wm^{-2}) = (0.43 Wm^{-2})(10^{12} m^{-3} / N_e)^3 (T_e / 1000K)^4 (f / 1.0GHz)^3 \tag{3.3}$$

where T_e is the electron temperature in the ionosphere. There is a caveat on equation (3.3) and that is that strictly there is no absolute threshold for triggering the instability. An assumption is made about how fast it needs to grow spatially along the beam direction under typical conditions. The threshold is much more sensitive to condition parameters than for either SBS or SRS. For typical conditions with an electron density of 10^{12} m^{-3} and an electron temperature of 1500 K, the power flux threshold for a 2.48 GHz pump is 33 W m^{-2}, which means that the TSI would be excited by the SPS beam. However, for a 5.8 GHz beam the threshold would be 422 W m^{-2} which would mean the TSI would probably not be excited. Also, if the electron density were to fall to 50% of the assumed value, the threshold would become 264 W m^{-2}, for the 2.48 GHz case, which is probably marginal for the SPS.

It should be pointed out that as the TSI develops, plasma density irregularities are excited and self-focussing of the EM beam occurs where the electron density is reduced. This further enhances the temperature and pressure in the depletions which has the effect of further depleting the electron density, hence the instability. Although it is difficult to calculate the detailed structure of the developed interaction, it has been estimated that the plasma density depletions will maximise at about 10% of the ambient density. However, this may lead to self-focussing which locally increases the EM power density by a factor of 10 (Duncan, 1981). It should also be pointed out that under these conditions of a strongly excited nonlinear self-focussing, the scale of the plasma density variations across the beam may be quite different from the scale of the beam cross-section itself. The beam may actually striate so that several regions of enhanced and depleted plasma density and EM power density may appear across it. This is an example of symmetry breaking which is

typical of nonlinear processes. These structures are non-stationary and usually quite unpredictable except possibly on a statistical basis.

3.4 Experimental tests of nonlinear effects

Since the 1960s when high power radio transmitters of sufficient power and directivity became available, the ionosphere has been utilised as a laboratory to study experimentally the kinds of instabilities outlined above and a number of ground-based high power radio facilities are now established at various sites around the world (Robinson, 1989). Among the most relevant studies with such facilities include those by Fejer et al. (1978) who reported the detection of stimulated Brillouin scattering using a powerful 50 MHz radar at Jicamarca in Peru. Numerous observations of thermal self-focussing have been reported, e.g. by Farley et al. (1983) using the high power facility at Arecibo, in Puerto Rico and by Basu et al. (1987), using the EISCAT high power facility in Tromsø, Norway. However, these results, although partly motivated by the earlier interest in the USA in SPS systems, are not entirely satisfactory due to the limitation of the operating frequencies of high power facilities involved to frequencies well below those of the SPS systems themselves. Although frequency and power scaling, guided by the simple relations (3.1) to (3.3) above, can be carried out the nonlinear development of the instability, well above threshold powers, may be quite different than expected from such relations.

The only direct observations carried out so far on the interaction of microwave beams of frequency and power density similar to those proposed for SPS systems are those from the MINIX (Microwave-Ionosphere Nonlinear Interaction eXperiment) experiment (Kaya et al., 1986). The MINIX experiment was carried out with the aid of a mother-daughter rocket system which was flown through the ionosphere. A 2.45 GHz transmitter on the mother section transmitted a beam of microwaves through the ionospheric plasma to a receiver on the separated daughter craft. A spectrum analyser operating in the MHz band was connected to the receiver. The results indicated that electrostatic plasma waves were excited by the stimulated Raman scattering mechanism dealt with in section 3. This is to be expected since the MINIX microwave beam had a power density of 230 W m^{-2}, which greatly exceeded the power threshold for the excitation of SRS given by relation (3.2). In addition, electrostatic waves other than the electron acoustic waves triggered in SRS were also observed. These were electron cyclotron waves that occur at a frequency close to the electron gyro-frequency, which is close to 1.5 MHz in the ionosphere. Unlike SBS and SRS above, no simple analytical treatment of electron cyclotron waves is possible. However, the MINIX team was able to successfully simulate the generation of the observed electron cyclotron waves using computer techniques (Matsumoto and Kimura, 1986). The MINIX wave detector's limitation to the MHz band meant it was incapable of detecting the ion acoustic wave products of SBS that propagate at much lower frequencies. Thus, the excitation of this instability during strong microwave transmissions through the ionosphere has yet to be directly established.

No evidence of thermal self-focussing was found in the MINIX experiment. However, this may not be too surprising since the heating in the upper ionosphere on which the TSI depends is largely controlled by gradients across the geomagnetic field. The relatively narrow microwave beams available on the MINIX rocket may have led to rapid transverse heat conduction out of the beam. Narrow beams would also be unlikely to excite self-

focussing effects because the plasma density inhomogeneities involved have larger scale sizes (100 m to 1 km) than the cross-section of the beam itself. Much broader beams in real SPS systems would not necessarily behave in the same manner.

The MINIX experiment also did not indicate any significant plasma heating due to the expected collisional absorption of microwave energy. This heating is one of the basic elements of the environmental impact effects that are dealt with in the following section. Kaya et al. (1986) explained the lack of evidence for such heating by noting that the electron temperature enhancements could have been below the (100 K) sensitivity of the measuring instruments. They also pointed out that the heating efficiency of the microwaves was reduced by the motion of the rocket which meant that the energy source could not remain long enough in the locally heated region to cause significant temperature increases. It is also likely that the effects mentioned above in the context of TSI excitation would also reduce the overall heating efficiency.

3.5 Summary of nonlinear effects

Threshold powers for nonlinear interactions involved in stimulated Brillouin scattering, stimulated Raman scattering and the thermal self-focussing instability have been presented in the context of the propagation of SPS microwave beams traversing the ionospheric plasma. All three of these processes have been found capable of being excited with the planned SPS power levels. These power levels greatly exceed the required levels for SBS and SRS but only marginally so for the TSI. Experimental evidence for the excitation of at least SRS has been found in the MINIX experiments and it is quite likely that SBS was also excited. Once the power threshold for these nonlinear interactions has been exceeded, then positive feedback effects lead to instability and the amplitudes of the waves excited in these processes grow unstably. The development of this nonlinear growth stage and its ultimate saturation is poorly understood. Strongly excited instabilities can lead to multi-wave mode excitation and turbulence. The plasma waves and irregularities that develop can strongly affect the SPS beam itself by scattering microwave energy into electrostatic waves so that some of its energy is lost in the ionosphere. This process is termed anomalous absorption. In addition the refractive variations caused by the TSI can cause self induced scintillation effects in the SPS beam itself. However, because of the uncertainty in the nonlinear development stage of the instabilities it is difficult to predict how big these effects might be in practice.

4. Environmental impact

The starting point for an investigation of the environmental impact of a high power microwave beam passing through the atmosphere is the heating of the electron gas in the ionosphere due to the collisional absorption effects treated in section 2.1. This heating increases the temperature of the electron gas and this in turn has a number of consequences for the plasma density and chemical content of the atmosphere at ionospheric heights, due to dependence of the rates of chemical reactions on the electron temperature. These changes in response to microwave heating in the context of SPS systems are outlined below.

4.1 Electron temperature enhancements

When a microwave beam is switched on in the ionospheric plasma, the absorption rate given by expression (2.2) gives rise to steady heating of the electron gas which initially causes its temperature to rise. As the electron temperature increases above that of the heavier neutral particles heat is lost to them. This process is represented by the following differential equation (Gurevich, 1978)

$$dT_e/dt = 2e^2\nu_e P/(3m_e\varepsilon_0 c\omega_0{}^2) - \delta\nu_e(T_e - T) \tag{4.1}$$

where t is time, P is the power density of the microwaves, T is the temperature of the neutrals and $\delta\nu_e$ is the rate of energy loss per electron. The first term on the right hand side of (4.1) represents the microwave heating and the last term is the cooling due to energy loss to the neutrals. Expression (4.1) is only valid in the absence of transport processes, such as thermal conduction and plasma diffusion. Such transport processes can often be neglected as long as the plasma remains uniform on scales of several kilometres. This will be the case in the SPS context for sufficiently wide beams and in the absence of TSI induced plasma density inhomogeneities. However, expressions of the same form as (4.1) may be useful even when the SBS and SRS processes are excited. The extra anomalous energy loss, in addition to the collisional type, can be accounted for by replacing ν_e by an anomalous collision frequency in the heating term (but not the loss term) in (4.1). However, the physics of the nonlinear development of the instabilities involved is subject to considerable uncertainty. Consequently the value of this anomalous collision frequency is difficult to ascertain. No attempt, in what follows, has been made to quantify any anomalous heating effects. This can only be addressed in a more detailed study. It is generally acknowledged that quantitative prediction in the case of strongly nonlinear phenomena is an exceedingly difficult problem.

It should also be noted that the collisional process that causes both the absorption and heating is entirely elastic. If the loss process was also through elastic collisions then the factor δ in (4.1) would simply be the ratio of the electron mass to the neutral mass, which is of the order of 10^{-5} in the ionosphere. However, the dominant loss process is through inelastic rather than elastic collisions. δ is then a much more complicated parameter which depends on the temperature of the electrons and neutrals and requires a detailed knowledge of the numerous types of inelastic interactions. Detailed parametric expressions for all of the relevant processes may be found in Schunk and Nagy (1978). Gurevich (1978) has reduced these details to a single T_e dependent curve that greatly simplifies estimations of electron heating effects. It turns out that for electron temperatures between around 800 K to 2000 K the value of δ is close to 10^{-3}, which is around two orders of magnitude larger than the value for elastic collisions.

If the microwave heating source is steady, as it would be in the SPS case, then the electron temperature quickly reaches an equilibrium value above that of the background neutrals. This may be found by setting the time derivative in (4.1) to zero which results in

$$T_e/T = 1 + P/P_T \tag{4.2}$$

where

$$P_T\,(Wm^{-2}) = (74.9Wm^{-2})(T/1000K)(f/1.0GHz)^2 \qquad (4.3)$$

The characteristic power density P_T in (4.2), for which heating effects are significant, has been cast in the same form as the instability threshold in expressions (3.1) to (3.3), for ease of comparison. Thus, at a microwave frequency of 2.48 GHz, with a typical neutral temperature of 1000 K at 200 km in the atmosphere, P_T is 460 W m^{-2}. This means that an SPS system with P = 100 W m^{-2} would cause an electron temperature increase of 217 K. This is consistent with values predicted by Perkins and Roble (1978), Perkins and Goldman (1981) and Duncan (1981) for earlier SPS proposals in the USA.

Perkins and Roble (1978) estimated electron temperature increases of up to 1000 K with a power flux of 500 W m^{-2} and an operating frequency of 3 GHz. They also included plasma transport effects and showed that the temperature enhancements would follow the geomagnetic field lines rather than the beam geometry, because of the previously mentioned effects of the geomagnetic field on electron transport. They also claimed that so called electron thermal runaway might occur in which electron heating would develop in an unlimited way. This effect was later shown to be due to incorrect transport coefficients (Duncan, 1981). In addition, Perkins and Goldman (1981) have demonstrated the possibility that SPSs could excite the TSI as discussed in section 3. Their results also indicate geomagnetically field aligned temperature perturbations of 1000 K or so. These effects have also been examined in detail by Duncan (1981). This tendency for plasma density changes to exhibit structure aligned to the magnetic field is a result of the anisotropic nature of electron transport in plasma in a magnetic field.

The results on SPS heating effects reported by Matsumoto (1981) are largely invalid because the loss processes used were incorrect. This author predicted very high electron temperature increases of around 7000 K with SPS operating parameters similar to those above. This is because only elastic collisional effects were taken into account in the electron loss process, whereas, as pointed out above, the dominant losses are due to inelastic collisions.

4.2 Electron density effects

Changes in the ionospheric electron density, as a result of electron temperature enhancements described above, occur in two broadly different ways. Firstly, changes can occur in the electron density due to the temperature dependence of the rate at which free electrons are lost due to recombination and attachment. It turns out that such processes always lead to electron density increases. Secondly, electron temperature increases lead to thermal electron gas pressure increases and if these contain gradients then plasma is pushed out of high pressure regions. This leads to electron density depletion. Which of these two processes dominates depends on the strength of the gradients, and also on altitude. For the scale size involved in SPS beams, it would be expected that recombination type chemistry will dominate over transport below about 200 km, whereas the opposite situation will occur above about 250 km. When depletions in electron density occur, the refractive properties of electromagnetic waves in plasma lead to focussing and increases in the electromagnetic

power density of the heating wave. This is the basis of the self-focussing instability described in section 3 above. Indeed the depletion situation is best regarded as the nonlinear development of the self-focussing instability. This cannot be treated in a simple analytical way and its detailed treatment is beyond the scope of the present report. In the other limit, where electron density increases arise, then defocusing follows. This is clearly a self-limiting process and usually rather weak in practice. This means that the recombination-dominated case can be treated analytically and this is done below.

At altitudes below 200 km where recombination type processes dominate, the electron density changes are found, to a good approximation, from the differential equation

$$dN_e/dt = q_i - \alpha(T_e)N_e{}^2 \tag{4.4}$$

where q_i is the ionisation rate due to solar photoionisation and $\alpha(T_e)$ is the electron temperature dependent recombination rate. $\alpha(T_e)$ is an average over various chemical species (see next subsection) and is approximately inversely proportional to T_e. Thus, assuming that the electrons are in thermal equilibrium with the background neutrals in the absence of the microwave heating, (4.4) predicts that the ratio of electron density at the heated electron temperature, to that at the unheated background temperature will be

$$N_e(T_e)/N_e(T) = (\alpha(T)/\alpha(T_e))^{1/2} \approx (1 + P/P_T)^{1/2} \tag{4.5}$$

where relation (4.2) has been used. Thus, using the example above i.e. a microwave frequency of 2.48 GHz, with a typical neutral temperature of 1000 K at 200 km in the atmosphere and with P = 100 W m^{-2}, which causes an electron temperature increase of 217 K, then the electron density would increase locally by close to 10%. By the same token, for a power density of 500 W m^{-2}, the density would increase by about 40%.

4.3 Ionospheric chemistry effects

In addition to the electron density increases due to recombination effects described above, the total ion density also increases to maintain the quasi-neutrality of the ionosphere. As implied above, the electron recombination rates are averaged over several chemical species. The main photoionisation processes that produce free electrons at altitudes between 100 to 200 km involve atomic and molecular oxygen and molecular nitrogen. This leads to the production of ions O^+, $O_2{}^+$ and $N_2{}^+$. A secondary process then quickly removes the $N_2{}^+$ and produces the commonly observed NO^+ ions. Under the action of microwave heating the change in the density of the main ions is then determined by the following set of coupled equations (Gurevich, 1978)

$$dN_{O_2{}^+}/dt = q_{iO_2{}^+} + \beta_2 N_{O_2} N_{O^+} - \alpha_2 N_{O_2{}^+} N_e \tag{4.6}$$

$$dN_{O^+}/dt = q_{iO^+} - \beta_1 N_{N_2} N_{O^+} - \beta_2 N_{O_2} N_{O^+} \tag{4.7}$$

$$dN_{NO^+}/dt = q_{iNO^+} + \beta_1 N_{N_2} N_{O^+} - \alpha_1 N_{NO^+} N_e \quad (4.8)$$

where q_{X^+} represents the production rate of ion X^+, α_1 and α_2 are electron temperature dependent rate coefficients and β_1 and β_2 are rate coefficients which are largely independent of electron temperature. Account has also been taken of the subsidiary reactions

$N_2 + O^+ \rightarrow NO^+ + N$ and $O_2 + O^+ \rightarrow O_2^+ + O$.

Details of the rate coefficients in (4.6) to (4.8) and their temperature dependences are given in Gurevich (1978). With the aid of these data, stable solutions of (4.6) to (4.8), together with (4.2) and (4.4) allow the changes in concentration for the various ion species to be calculated for a given microwave power density. These changes are, as expected, of similar size to the corresponding changes in N_e in (4.5).

At altitudes below 100 km, the chemical interactions become more complex due to the increasing density of minor species and the enhanced reaction rates of some weaker reactions in the presence of higher molecular concentrations. A detailed treatment of this complex situation is beyond the scope of the present summary, but suffice it to say that the basic mechanisms are similar to those described above; they just involve more coupled rate equations of the type (4.6) to (4.8). More details may be found in Tomko et al. (1980).

One of these lower altitude effects that may be worth a further comment here, because of its role in the wider environmental context, is that of ozone production. This occurs, again in response to electron heating, through a multi-stage process which is initiated by the production of negative oxygen molecular ions. Several subsequent stages are possible. One such multi-stage process is

$e^- + O_2 + O_2 \rightarrow O_2^- + O_2 \rightarrow O_3 + e^-$

The rate for the initial stage of this process is (Tomko et al., 1980)

$$1.4 \times 10^{-30} (300K/T_e) \exp[(100K/T) - (700K/T_e)](N_{O_2})^2] \text{ m}^{-3}\text{ s}^{-1} \quad (4.9)$$

The rate for the second stage does not involve electron heating and is just (Tomko et al., 1980)

$$3.0 \times 10^{-13} N_{O_2^-} N_O \text{ m}^{-3}\text{ s}^{-1} \quad (4.10)$$

A precise evaluation of the rate of production of ozone by this and alternative processes listed by Milikh and Duncan (1991) requires the solution of a combination of coupled rate equations similar to (4.6) to (4.8) and is beyond the scope of the present survey. In principle, such effects could also be caused by SPS beams, although as long as the SPS power density P can be kept to values which do not exceed P_T above, then the changes in

relative concentration through electron heating should be no more than a fraction of a percent.

4.4 Neutral temperature effects

As a side effect of the heating of electrons, weak indirect heating of the neutral gas also occurs through the collisional loss process included in equation (4.1) (Robinson, 1996). After the electron temperature reaches its new equilibrium value above that of the neutral gas (4.2) due to microwave heating, all of the heat energy that is transferred from the microwaves to the electron gas goes into the neutral gas, which acts as a heat sink. However, in the inelastic collisions most of the energy lost to the neutrals by the electrons goes into exciting the bound electrons in the neutral atoms or molecules. This energy is quickly radiated as photons and as a result, the net transfer of thermal energy from the electrons to the neutrals is that expected from elastic collisions. Thus, the neutral temperature, T increases at a steady rate given by

$$dT / dt = \delta_0 \nu_e (N_e / N_n)(T_e - T) = \delta_0 \nu_e N_e P T / (N_n P_T) \qquad (4.11)$$

where δ_0 is the ratio of the electron to the neutral mass and N_n is the neutral gas concentration. Now N_n is around 10^{16} m^{-3} at 200 km altitude and δ_0 is around 10^{-5}. Thus, with the values of other parameters in (4.11) set to those used in the previous calculations above, the rate of increase of the neutral gas temperature for SPS power densities of 100 W m^{-2} would be approximately 2.0×10^{-4} K s^{-1}. This means that the neutral temperature would increase by about 1 K every hour in the SPS beam. In practice the neutral temperature would not keep increasing at this rate. A variety of thermal loss effects would limit the neutral temperature increases. Probably the most effective of these loss processes is advection due to prevailing horizontal neutral winds. These have values of 10 to 100 m s^{-1} at altitudes below 100 km. For example, a wind of 10 m s^{-1} blowing across an SPS beam of width 10 km would limit the neutral temperature increases to around 0.2 K. This would increase to 1 K if the SPS power density was increased from 100 to 500 W m^{-2}.

One consequence of the heating of the neutral gas would be a change in ozone concentration in the lower ionosphere. This can be inferred from a model first suggested by Chapman. It leads to a reduction in ozone concentration for increases in the neutral temperature given by (Milikh and Duncan, 1991)

$$\Delta N_{O_3} / N_{O_3} = (1330\text{K}/T)(\Delta T / T) \qquad (4.12)$$

where $\Delta N_{O_3} / N_{O_3}$ and $\Delta T/T$ are the relative changes in ozone concentration and neutral temperature, respectively. Thus, on this basis, the change of 0.2 K in the neutral temperature with a background of 1000 K, due to SPS microwave heating, found above, would lead to a relative change of 0.026% in the ozone concentration. This would increase to 0.1 % if the SPS power density were increased from 100 to 500 W m^{-2}. These are clearly exceedingly small values for ozone concentration changes brought about by this process in the context of SPS.

4.5 Impact on telecommunications

Rush (1981) has pointed out the effects of the SPS induced ionospheric temperature and plasma density perturbations and has concluded that there could be significant interference due to absorption, scattering and scintillation with trans-ionospheric radio signals associated with communication, navigation and commercial broadcasting systems. Firstly, increases in electron temperature cause increases in the temperature dependent collision frequency ν_e. This in turn increases the absorption coefficient, through relation (2.2) of any signal passing through a region of the ionosphere heated by the SPS beam. This relation also indicates that the increases in electron density, outlined above, that accompany the temperature increases will lead to a further enhancement of the absorption coefficient. The temperature dependence of ν_e on T_e is given approximately by

$$\nu_e(T_e)/\nu_e(T) = T_e/T \tag{4.13}$$

Given the relative changes in electron temperature and plasma density of 20% and 10% respectively, estimated above for a SPS power density of 100 W m^{-2}, (4.13) would imply an increase of up to 30% in the dB level of the absorption (relation 2.1) for a signal passing through a layer of ionosphere that was completely heated by the SPS beam. This effect also occurs for the SPS beam itself, although at the SPS frequencies it is a negligible increase. However, for public broadcasting stations that have frequencies in the HF band and that pass through the heated region, the effect could be considerable, since the absorption coefficient increases with the inverse square of the signal frequency (see relation 2.2). At a typical HF frequency of 6 MHz the natural absorption levels can be 10 dB or higher. The effect of SPS heating would increase the 10dB value to 13dB, which is a doubling of the power loss through absorption.

In addition to the enhancement of these collisional absorption effects, it is possible that the generation of electrostatic waves by the nonlinear processes of stimulated Brillouin and Raman scattering described in section 3 could lead to further losses in signals traversing the SPS affected region of the ionosphere. This occurs over a wide range of frequencies and is due to scattering from the plasma density irregularities associated with the electrostatic waves created by the SPS through SBS and SRS. Further, if the thermal self-focussing effects are excited then this will cause scintillations in signals traversing the SPS affected region. These effects can be strong if the nonlinear effects are strongly excited, but as with the other nonlinear processes touched on above, great uncertainty attaches to any quantitative estimate of such effects.

5. Data Sources

A variety of data sources and models exist which will be of central importance in determining the atmospheric impact to and from solar power satellites. In particular profiles of electron density as a function of altitude and on a global scale are essential for assessing the effects discussed above. Below some of the key sources of data are outlined.

(i) The international reference Ionosphere (IRI)

(http://nssdc.gsfc.nasa.gov/space/model/models/iri.html).

This provides a global model of electron density, electron temperature, ion temperature, ion composition (O^+, H^+, He^+, NO^+, O_2^+), ion drift, TEC. It is freely available from the NASA/GSFC NSSDC, both as source code and web-based plotting. This model is widely used in radio propagation prediction (e.g. voacap). It provides input for e.g. ionospheric absorption calculations. Figure 5 shows an example of a global map of total electron content (TEC) derived from the IRI.

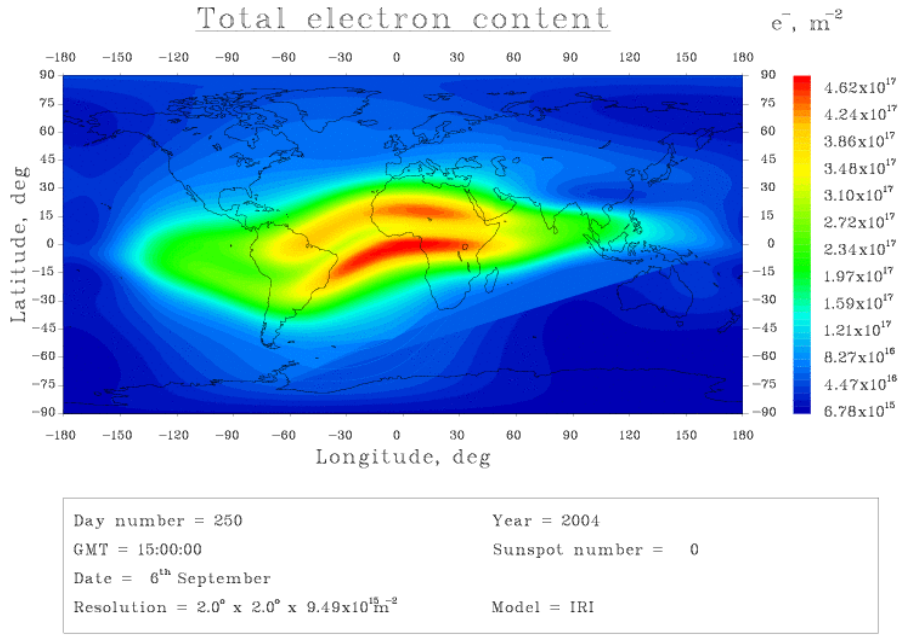

Figure 5. Example of global total electron content output from the International Reference Ionosphere

(ii) The Mass-Spectrometer-Incoherent-Scatter (MSIS) model

(http://nssdc.gsfc.nasa.gov/space/model/atmos/msise.html)

This is the equivalent to the IRI for the neutral upper atmosphere and is also freely available from the NASA/GSFC NSSDC. Enables the computation and plotting of neutral temperature, exospheric temperature, densities of He, O, N_2, O_2, Ar, H, and N, and total density.

Both these models provide excellent typical values. However they poorly represent extreme events, and average over variable events, and thus are limited in providing anything other than average performance indicators.

Local bottom-side ionospheric profiles (i.e. below the electron density peak) may be detailed more accurately for extreme and time variable events via an extensive global network of ionosondes (Figure 6). Data acquisition is on a fairly ad-hoc basis, and the application of meteorological-style data assimilation techniques could improve this if required for SPS operations. In addition, dual frequency altimeter systems such as TOPEX/Poseiden have provided valuable global maps of TEC over a modest timescale. A

global network of Riometers also exist, which can provide direct measurements of ionospheric absorption at ~40 MHz, which can be scaled to SPS frequencies.

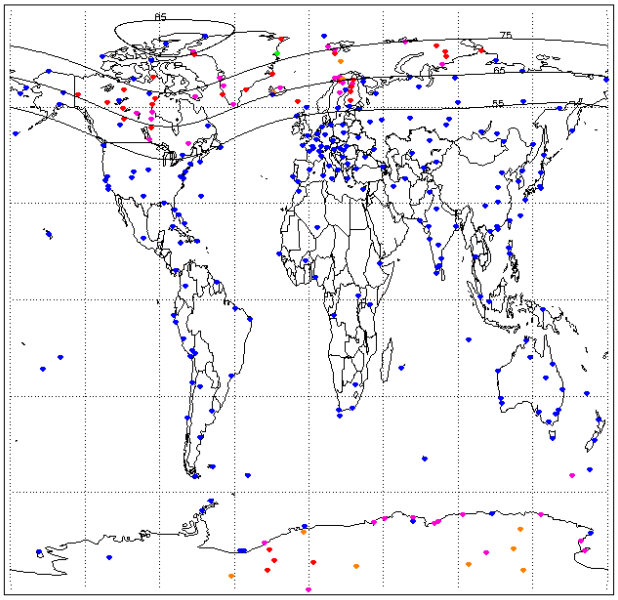

*Figure 6. Global distribution of ionosonde and riometer sites (*http://www.wdc.rl.ac.uk/gbdc/iono_riom.html

Accurate measurements of all ionospheric parameters required for the calculation of, for example, an absorption profile requires more sophisticated instrumentation such as an incoherent scatter radar. A modest number of such facilities currently exist:

High latitude: The EISCAT Svalbard radar
Auroral latitudes: The EISCAT VHF and UHF (Norway), the Søndre Strømfjord radar (Greenland).
Mid latitudes: The Millstone Hill observatory (USA), the MU radar (Japan)
Low latitude: The Arecibo Observatory (Puerto Rico)
Equatorial latitudes: The Jicamarca Radio Observatory (Peru)

6. Limitations to current knowledge, recommendation for further work and conclusions

Above the key mechanisms involved in the propagation of Solar Power Satellite microwave beams through the ionospheric plasma have been outlined. These include absorption, scintillation and nonlinear interaction processes which can lead to reduced transfer efficiency of energy from the SPS platform to receivers on the ground. In addition, effects which lead to modification of the Earth's aerospace environment through heating of ionospheric electrons by the absorption of SPS microwave energy have been outlined. The main consequences of this heating are increases in the electron and neutral gas temperature and changes in the electron density and concentrations of the various ions and neutral components of the atmosphere at ionospheric heights.

The accuracy of quantitative predictions of the size of these effects depends on a number of factors. The most important are an understanding of the physical mechanisms involved, quantitative knowledge of relevant parameters that occur in the mathematical relations, the natural variability of the atmosphere and ionosphere and the intrinsic unpredictability of the nonlinear effects. The linear absorption and scintillation processes outlined in section 2 are relatively well understood and quantitative predictions of these effects are probably quite reliable, as are the chemical rate coefficients involved in environmental impact changes in section 4. However, the natural variability of the ionosphere, as well as the fundamental unpredictability of nonlinear effects certainly limit the accuracy with which the performance of SPS systems and their environmental impact can be estimated. If nonlinear effects are strongly excited so that anomalous energy absorption arises, in addition to linear collisional absorption, then the microwave heating from which all the other effects discussed above follow could be considerably higher than expected, resulting in correspondingly higher levels of self absorption and environmental impact.

Of those processes considered in this report, the effects of diffractive scintillations, due both to naturally occurring ionospheric plasma density irregularities, as well as those which can be excited by the SPS beam itself, through the thermal self-focussing instability, probably give rise to the most cause for concern with regard to detrimental effects. Observations already carried out on existing satellite-ground links indicate that natural amplitude fluctuations of close to 100% may occur on 2.48 GHz signals, with somewhat smaller fluctuation levels on 5.8 GHz. These are large variations compared to the effects of collisional absorption which can occur under certain extreme condition (see section 2.1). There exist reasonably complete statistics on the occurrence of scintillation effects from data sources such as those mentioned in section 5. Occurrences are related to the state of the solar-terrestrial environment (space weather). However, it must be stressed that severe events of this nature are largely unpredictable, although sometimes early warnings are possible on time scales ranging from a few minutes to several hours if space-based monitoring data are available. However, in the case of self-induced scintillation effects through the TSI, there may be no way of avoiding significant power amplitude fluctuations. As pointed out above, scintillation effects are accompanied by scattering of some proportion of the microwave power out of the geometrical beam which could mean microwave power impacting on the ground outside the receiving antenna area. From estimations based on the models mentioned in section 2, these power fluctuations might be expected to occur at radii as much as 5 km greater than that of a geometrical SPS beam.

There exist detailed studies, albeit over twenty years old, of the potential environmental impact of SPS transmissions through the ionosphere. Most of these relate to the heating of the ionosphere as indicated in section 4 above. There has been less emphasis on the detrimental effects of the ionosphere on the SPS beam itself. It would be highly desirable both to update the previous studies on environmental effects by including new space weather data acquired over the last two decades as well as improved computer modelling methods, in addition to carrying out systematic studies into the effects on the SPS beam. Further research should consist of three strands. Firstly a study of occurrences of scintillation events with specific emphasis on inferring operating efficiency statistics for specific SPS locations is needed. Secondly, a programme of computer modelling of the TSI should be undertaken, to improve understanding of its excitation by SPS systems and

especially to predict, as far as possible, the nonlinear evolution of the SPS ionosphere interaction. Such a study would also lead to improvements in our ability to predict environmental impact effects of SPS systems.

Finally, it is also essential to carry out further experimental studies of microwave-plasma interactions. The single small scale MINIX study reported by Kaya et al., 1986 is a rather inadequate basis for inferring the behaviour of a full scale SPS system for various reasons indicated in section 3 above. The MINIX results did indicate that plasma waves were excited by the stimulated Raman scattering mechanism, but other important effects such as stimulated Brillouin scattering, plasma heating and nonlinear self-focussing, which are expected from theory and which could have important consequences for both the operating efficiency of the SPS system and the impact on the environment, were not detected. The reasons for this have been discussed above. In particular, the narrow microwave beams used on the MINIX would also be unlikely to excite self-focussing effects. Much broader beams in real SPS systems would not necessarily behave in the same manner. It would seem essential therefore, that experiments should be conducted on spatial scales which better match those that will be encountered in any future SPS system. It may be possible to carry out such experiments with suitable ground based high power radio transmitters in the first instance. Otherwise some large space platform would have to be utilised for large scale experimental studies in space.

7. References

Basu Sa, Su Basu, P Stubbe, H Kopka and J Waarmaa, Daytime scintillation induced by high-power HF waves at Tromsø, Norway, **J. Geophys. Res**., 92, 11149-11157, 1987.

Basu Sa, E Mackenzie and Su Basu, Ionospheric constraints on VHF/UHF communications links during solar maximum and minimum periods, **Radio Sci**., 23 363, 1988.

Davies K, **Ionospheric Radio**, IEE, 1990.

Duncan LM, SPS environmental effects on the upper atmosphere, **Space Solar Power Rev**., 2, 87-101, 1981.

Farley DT, C LaHoz and BG Fejer, Self-focusing instability at Arecibo, **J. Geophys. Res**., 88, 2093-2102, 1983.

Fejer JA, Ionospheric modification and parametric instabilities, **Rev. Geophys. Space Phys**., 17, 135-153, 1979.

Fejer JA, K Rinnert and R Woodman, Detection of stimulated Brillouin scattering by the Jicamarca radar, **J. Geophys. Res**., 83, 2133-2136, 1978.

Glaser PE, FP Davidson and KI Csigi, **Solar Power Satellites**, John Wiley, 1998.

Gurevich AV, **Nonlinear Phenomena in the Ionosphere**, Springer, 1978.

Inan US , TF Bell and JV Rodriguez, Heating and ionization of the lower atmosphere by lightning, **Geophys. Res. Lett**., 18, 705-708, 1991.

Kaya N, H Matsumoto, S Miyatake, I Kimura, M Nagatomo and T Obayashi, Nonlinear interaction of strong microwave beam with the ionosphere MINIX rocket experiment, **Space Power**, 6, 181-186, 1986.

Matsumoto H, Numerical simulation of SPS microwave impact on ionospheric environment, **Acta Astronatica**, 9, 493-497, 1982.

Matsumoto H and T Kimura, Nonlinear excitation of electron cyclotron waves by a monochromatic strong microwave, **Space Power**, 6, 187-191, 1986.

Milikh GM and LM Duncan, Radio wave effects on atmospheric ozone, in **Controlled Active Global Experiments(CAGE)**, E Sindoni and AY Wong (eds.) , SIF Bologna, pp227-238, 1991.

Ogawa T, K Sinno, M Fujita and J Awaka, Severe disturbances of VHF and GHz waves from geostationary satellites during magnetic storms, **J. Atmos. Terr. Phys**., 42, 637, 1980.

Perkins FW and RG Roble, Ionospheric heating by radio waves: Predictions for Arecibo and the Satellite power station, **J. Geophys. Res**., 83, 1611-1624, 1978.

Perkins FW and MV Goldman, Self-focussing of radio waves in an underdense ionosphere, **J. Geophys. Res**., 86, 600-608, 1981.

Robinson TR, Modification of the high latitude ionosphere by high power radio waves, **Physics Reports**, 179, 79-209, 1989.

Robinson TR, Modification of the ionosphere by high power radio waves, **Science in Parliament**, 53, 19-20, 1996.

Robinson TR and R Leigh, An evaluation of the ionospheric correction for the ERS-1 Altimeter, **IEE Antennae and Propagation Conf. Proc.**, Pub. No 274 pt 2, pp 57-59, 1987.

Robinson, TR and R Beard, A comparison between electron content deduced from the IRI and that measured by the TOPEX dual frequency altimeter, **Adv. Space Sci.**, 16, (1)155-(1)158, 1995.

Rush CM, SPS simulated effects of ionospheric heating on the performance of telecommunication systems: a review of experimental results, **Space Solar Power Rev**., 2, 355-366, 1981.

Schunk RW and AF Nagy, Electron temperatures in the F region of the ionosphere: Theory and observations, **Rev. Geophy. Space Phys**., 16, 355, 1978.

Summerer L, M Vasile, R Biesenbroek and F Ongaro, Space and ground based large scale power plants: A European perspective, IAC-03/R.1.09, 2003

Tomko AA, AJ Ferraro and HS Lee, A theoretical model of D-region ion chemistry modifications during high power radio wave heating, **J. Atmos. Terr. Phys.**, 42, 275-285, 1980.

Wong AY, J Steinhauer, R Close, T Fukuchi and GM Milikh, Conservation of ozone in the upper atmosphere by ion removal, **Comments Plasma Phys. Controlled Fusion**, 12, 223-234, 1989.

Yeoman TK, MD Burrage, M Lester, TR Robinson and TB Jones, Long term variation of radar-auroral backscatter and the interplanetary sector structure, **J. Geophys. Res.**, 95, 21 123, 1990.

8. Acronym list

CME	Coronal Mass Ejection
EISCAT	European Incoherent Scatter
EM	Electromagnetic
ES	Electrostatic
GSFC	Goddard Space Flight Center
IRI	International Reference Ionosphere
MINIX	Microwave-Ionosphere Nonlinear Interaction eXperiment
MSIS	Mass Spectrometer Incoherent Scatter
NASA	National Aeronautics and Space Administration
NSSDC	National Space Science Data Center
SBS	Stimulated Brillouin Scattering
SPS	Solar Power Satellites
SRS	Stimulated Raman Scattering
TEC	Total Electron Content
TOPEX	TOPography EXperiment for Ocean Circulation
TSI	Thermal Self-focussing Instability
VHF	Very High Frequency
UHF	Ultra High Frequency

Appendix: The Ionosphere

The ionising action of the solar radiation on the upper atmosphere produces free electrons. Above about 60 km the number of these free electrons is sufficient to affect the propagation of electromagnetic waves. This "ionised" region of the atmosphere is a plasma and is referred to as the *ionosphere*. Longer wavelength radio signals reflect from the ionosphere. Shorter wavelength radio signals pass through the ionosphere but are affected by it, via processes such as absorption and scintillation.

Solar radiation passing through the atmosphere is absorbed and causes ionisation. This absorption means less radiation reaches the lower levels of the atmosphere and the level of ionisation is reduced. The density of the atmosphere decreases with height. This means there is less gas to ionise and so there is less ionisation. This results in a peak in the level of ionisation described by a "Chapman function". The real ionosphere is more complicated than this. The earth's atmosphere comprises several gases. Up to about 100 km the gases are well mixed due to turbulence and therefore have similar relative densities as at the surface. Above this height (which is referred to as the *turbopause*) the gases are in diffusive equilibrium and the vertical distribution of each gas is dependent on its molecular weight. Such complexities in ionospheric chemistry lead to substructure in the ionospheric profile, and the ionosphere has consequently been sub-divided into a number of layers, D, E, F1 and F2, depending on the layer characteristics. The D layer is highly collisional, characterised by complex chemistry, and the strong absorption of electromagnetic waves. The E layer is the main current-carrying layer, and the F layer represents the peak in electron density.

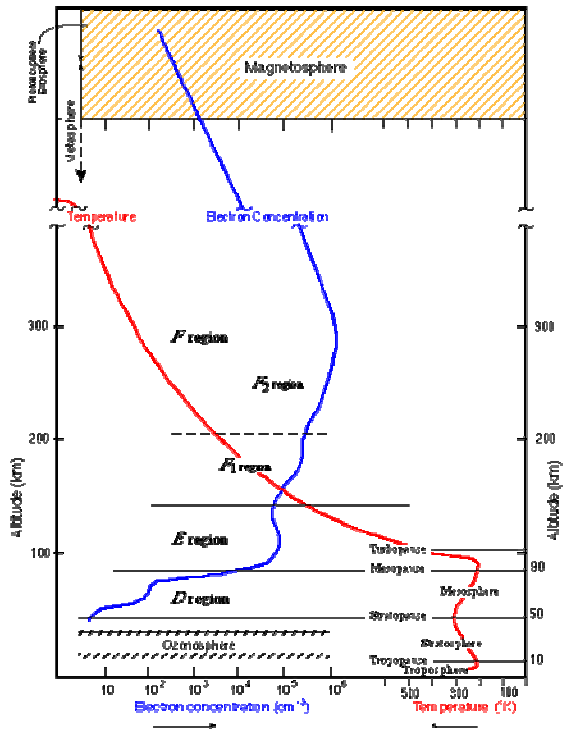

Figure A1 A typical daytime profile of electron concentration on which are marked the different layers of the ionosphere and the neutral atmosphere. A typical temperature profile is also shown.

Ionisation is not only caused by photoionisation, but also results from high energy particle precipitation. The amount of ionisation produced in this way is generally less than that produced by electromagnetic radiation. However, at night when there is little or no solar illumination, at times of high magnetic activity, and at the lowest altitudes where electomagnetic radiation cannot reach, the ionisation produced by charged particles is important.

The plasma density is a balance between the rate at which electrons are produced and the rate at which they are lost. The electrons are lost mainly in three ways: transport, recombination and diffusion. Recombination processes may be either radiative or dissociative, and reaction rates are highly temperature dependent. The combined effects of the production and loss rates lead to the observed ionospheric electron density profile.

In the E region the peak of production is at around 110-115 km. Plenty of molecular gas is present at this height so molecular ions are produced directly and the loss rate is controlled by dissociative recombination. This is not height dependant and so the resulting electron concentration in the E region closely resembles the production profile.

In the F region the peak of production is at around 150-160 km. but the peak of the electron concentration is well above this at around 250-300 km. Through the F region the loss rate gradually becomes controlled by the ion-atom exchange rate and this rate decreases with increasing height. In fact this loss rate falls away faster than the rate of production so the electron concentration actually increases. The reason that a maximum is reached is that plasma diffusion gradually takes over and the electron concentration is distributed in a similar way to the neutral gas concentration.

The height at which the transition from dissociative to ion-atom exchange controlled loss occurs can vary. If it is above the peak of production, then there will be a reduction in the actual electron concentration above the peak of production until ion-atom exchange loss takes over. This results in a ledge or secondary peak, the F1 layer, in the electron concentration profile at the peak of production.